JOURNAL OF CHEMICAL INFORMATION AND MODELING

Article

pubs.acs.org/jcim

Molecular Dynamics Simulations for Human CAR Inverse Agonists

Johanna Jyrkkärinne,* Jenni Küblbeck, Juha Pulkkinen, Paavo Honkakoski, Reino Laatikainen, Antti Poso, and Tuomo Laitinen*

University of Eastern Finland, Faculty of Health Sciences, School of Pharmacy, P.O. Box 1627, FI-70211 Kuopio, Finland

Supporting Information

ABSTRACT: Constitutive androstane receptor (CAR), along with pregnane x receptor (PXR), is an important metabolic sensor in the hepatocytes. Like all other nuclear receptors (NRs), CAR works in concert with coregulator proteins, coactivators, and corepressors which bind to the NRs. The main basis for the receptor to distinguish between coactivators and corepressors is the position of the C-terminal helix 12 (H12), which is determined by the bound NR ligand. CAR, having constitutive activity, can be repressed or further activated by its ligands. Crystal structure of human CAR bound to an agonist and a coactivator peptide is available, but no structural information on an inverse agonist-bound human CAR and a corepressor exists. In our previous molecular dynamics (MD) studies, no corepressor peptide was included. Therefore, probably due to the strong interactions which keep the relatively short H12 of CAR in the active position, the structural changes elicited by inverse agonists were very subtle, and H12 of CAR seemed to more or less retain its active conformation. Here, we have run a series of MD simulations to study the movement of H12 in the presence of both activating and repressing ligands as well as a corepressor peptide. The presence of the corepressor on the coregulator surface of CAR induced a clear shift of H12 of the inverse agonists-bound CAR. In general, H12 moved toward H10 and not away from the ligand binding domain, as seen in some other NRs. However, H12 of CAR is short enough that this movement seems to be adequate to accommodate the binding of the corepressor.

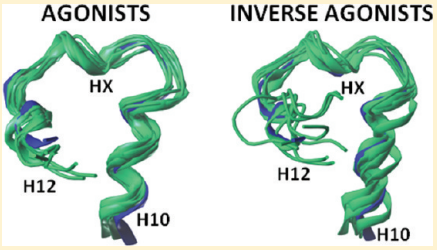

INTRODUCTION

Nuclear receptors (NRs) are ligand-dependent transcription factors that can bind to specific DNA elements on the promoter sites of their target genes and thereby regulate gene expression. The constitutive androstane receptor (CAR) is one of several NRs that act as metabolic sensors. CAR has a large and diverse set of endogenous and exogenous ligands that include environmental pollutants, many prescription drugs, and steroid hormones.[1] CAR's target genes encode both the metabolizing enzymes and transport proteins that are important for the elimination of both xenobiotic and endogenous compounds. In addition to xenobiotic metabolism, it has become evident that CAR also has a role in several physiological processes, such as energy metabolism and the metabolic conversion of heme, bilirubin, bile acids, and thyroid hormone.[2]

To be active, NRs need the help of different coregulator proteins, termed coactivators and corepressors.[3] Upon ligand binding, the conformation of the NR ligand binding domain (LBD) changes, the most important switch for activation/inactivation being the position of C-terminal helix, H12. In its active position, H12 forms a groove together with residues from helices 3 and 4, where the coactivators bind with their specific amino acid motif resembling LxxLL. Co-repressors have an overlapping binding site with coactivators; however, they have a longer binding motif (LxxI/HxxxI/L) than coactivators. Therefore, displacement of H12 is a prerequisite for corepressor binding.[3] Pure antagonists and inverse agonists usually have a bulky side chain that sterically pushes H12 away from its active position, thereby preventing coactivator binding. Some antagonists/inverse agonists (so-called passive antagonists) lack the bulky side chain, yet they fail to stabilize the active conformation of H12.[3,4]

CAR has quite a large ligand binding pocket (LBP) and, thus, can recognize a wide spectrum of ligands.[1] Another special feature of CAR is its constitutive activity: H12 can maintain its active position in the absence of any ligand. Therefore, ligand binding to CAR may result in agonism or inverse agonism. Furthermore, the same ligand may be able to recruit either coactivators or corepressors, and the net CAR activity depends on the pool of coregulators available in the cell.[5]

The exact mechanism of inverse agonism for CAR remains partially unclear. Only two agonist-bound but no inverse agonist-bound human CAR (hCAR) crystal structures exist.[6] For mouse CAR (mCAR), one inverse agonist-bound crystal structure with androstenol ligand exists,[7] but no coregulator peptides are included in it. Due to the species differences,[1] direct extrapolation of the information obtained from that crystal structure to human CAR is not possible because the identity in the human and mouse CAR LBD sequences is only 72%. Many of these differences are in the LBP, making it approximately 100 Å^3 smaller in mCAR than in hCAR and causing considerable differences in the ligand specificity. Also, the interactions between H12 and LBD are different.

We have previously reported on novel agonists and inverse agonists for CAR and studied their molecular mechanisms by

Received: September 13, 2011
Published: January 11, 2012

dx.doi.org/10.1021/ci200432k | J. Chem. Inf. Model. 2012, 52, 457−464

Table 1. Studied Ligands, Their *in Vitro* Activities, and Calculated Protein−Ligand Interaction Energies

ligand[a]	act[b]	NCoR act[c]	$E_{prot\text{-}lig/1ns}$	$E_{prot\text{-}lig/9ns}$
CITCO*	17.6 ± 2.5	2.2 ± 0.4	−53.3	−53.8
FL-82*	14.2 ± 2.3	1.0 ± 0.3	−31.1	−31.6
FL-81*	9.7 ± 4.5	1.5 ± 0.1	−39.7	−36.6
Permethrin*	9.2 ± 2.3	2.7 ± 0.3	−45.6	−44.9
Clotrimazole*	6.2 ± 1.5	4.9 ± 0.3	−34.2	−34.2
TPP*	3.5 ± 0.5	2.7 ± 0.3	−31.6	−31.2
Artemisin*	2.1 ± 0.7	2.6 ± 0.6	−30.8	−31.4
EE2**	0.1 ± < 0.1	1.5 ± 0.1	−35.0	−35.6
Androstanol**	0.5 ± < 0.1	19.1 ± 1.0	−42.1	−39.3
Androstenol**	0.2 ± < 0.1	9.7 ± 1.2	−40.3	−37.0
PK11195**	0.6 ± 0.1	23.8 ± 3.7	−41.9	−44.6
S07662**	0.4 ± 0.1	20.9 ± 10.2	−40.2	−34.5
Clomifene**	0.4 ± < 0.1	0.6 ± < 0.1	−52.4	−55.4
Celecoxib**	0.6 ± 0.1	0.7 ± 0.1	−33.8	−37.7
Meclizine**	1.6 ± 0.8	0.9 ± 0.1	−52.1	−51.7

[a]agonist*, inverse agonist**. CITCO: imidazo[2,1-b]thiazole-5-carboxaldehyde, 6-(4-chlorophenyl)-, O-[(3,4-dichlorophenyl)methyl] oxime. TPP: triphenyl phosphate. EE2: ethinylestradiol. [b]Activity at 10 μM concentration (for CITCO 1 μM) measured in reporter gene assays in mammalian cells, expressed as relative to solvent control ± s. d. [c]NCoR recruitment at 10 μM concentration (for CITCO at 1 μM, and for steroids EE2, androstenol, and androstanol at 30 μM) in mammalian two-hybrid assays, expressed as relative to solvent control ± s.d. No significant toxicity was seen with any of the compounds (see Table S1, Supporting Information).

using both biological and computational methods.[8−16] In the computational studies, we have created a quantitative structure activity relationship (QSAR) for CAR agonists and have applied molecular dynamics (MD) simulations and theoretical interaction energy calculations (MM-GBSA) to CAR ligands. However, the lack of protein flexibility in ligand docking,[11,12] the short length (1 ns) of the MD simulations,[15] and/or the absence of a coregulator peptide in MDs[16] have prevented us from clearly distinguishing between features for agonists and inverse agonists *in silico*.

In the present work, we wanted to test whether the presence of a corepressor peptide would elucidate more clearly the differences between agonists and inverse agonists in MDs. We docked both agonists and inverse agonists into CAR LBP and subsequently ran 10 ns MDs with a corepressor peptide from the silencing mediator for retinoid or thyroid hormone receptors (SMRT). SMRT is the only corepressor peptide which has been crystallized. The nuclear receptor corepressor 1 (NCoR), which has been used in the biological assays, has no crystal structures with NRs. However, since NcoR and SMRT both act in a similar fashion and require a larger binding groove than coactivators on the NR LBD, we used SMRT in the MDs. From these MDs, we analyzed the stability of different regions of the CAR LBD and calculated interaction energies at two time frames by using the MM-GBSA method.

EXPERIMENTAL SECTION

Ligand Docking. The dockings were performed with the GOLD docking suite (version 4.0; Cambridge Crystallographic Database: Cambridge, U.K., 2008). Ligands were docked into the human CAR LBD (crystal structure 1XVP, chain D), and the docking site was defined in GOLD by using the ligand molecule (CITCO) extracted from the crystal structure with a 10 Å distance for the ligand atoms. Side chains of F161 and

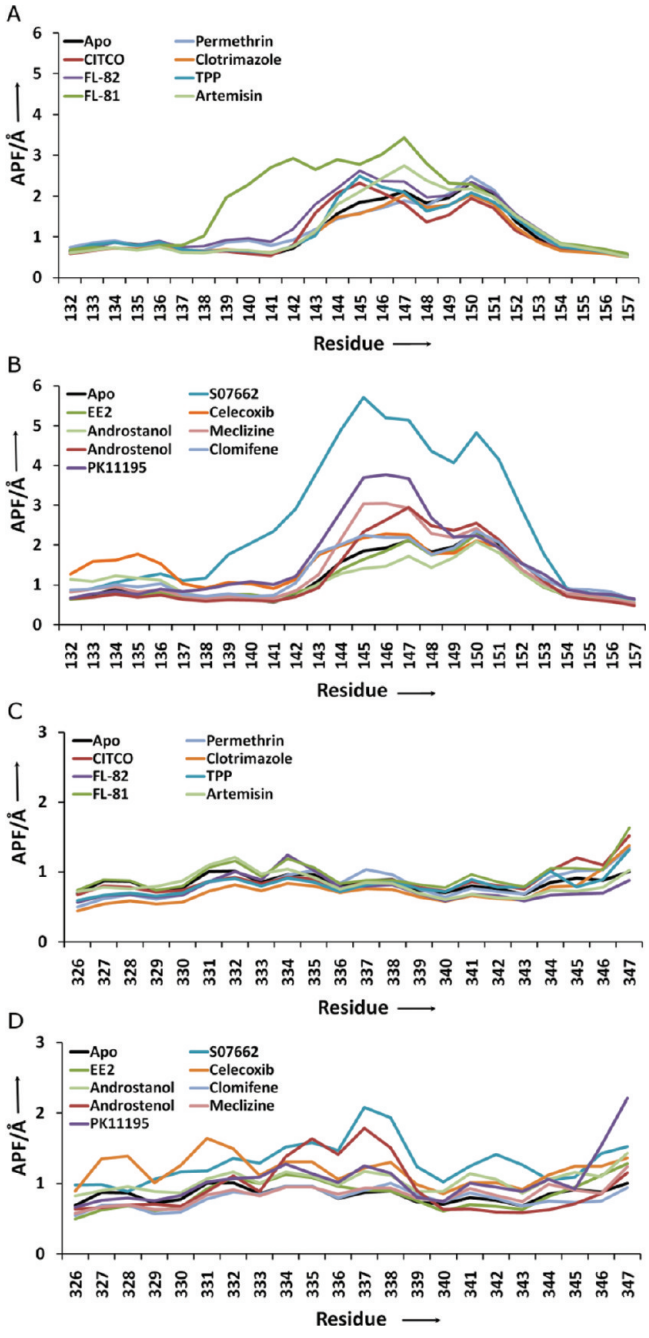

Figure 1. APF of the backbone atoms of hCAR during 10 ns MD simulations. H2−H3 loop in the presence of (A) agonists and (B) inverse agonists. APF of the C-terminal residues in the presence of (C) agonists and (D) inverse agonists.

Y224 were selected as freely moving side chains, according to previous MD simulations.[12] The maximum number of allowed poses was 10, and Goldscore was used as a scoring function. Otherwise, default settings were used. In the cases where the best pose could not be selected on the basis of the Goldscore and visual inspection, rescoring of the poses was performed by calculating binding energies (single point MM-GBSA energies) of ligands by using the standard MM-GBSA method as implemented in AMBER10.[17] For each pose, the coordinates of the complexes were taken from docking results, and the parameters were generated using the *tleap* module of AMBER10. The coordinates for the protein, the ligand, and the complex were

dx.doi.org/10.1021/ci200432k | J. Chem. Inf. Model. 2012, 52, 457−464

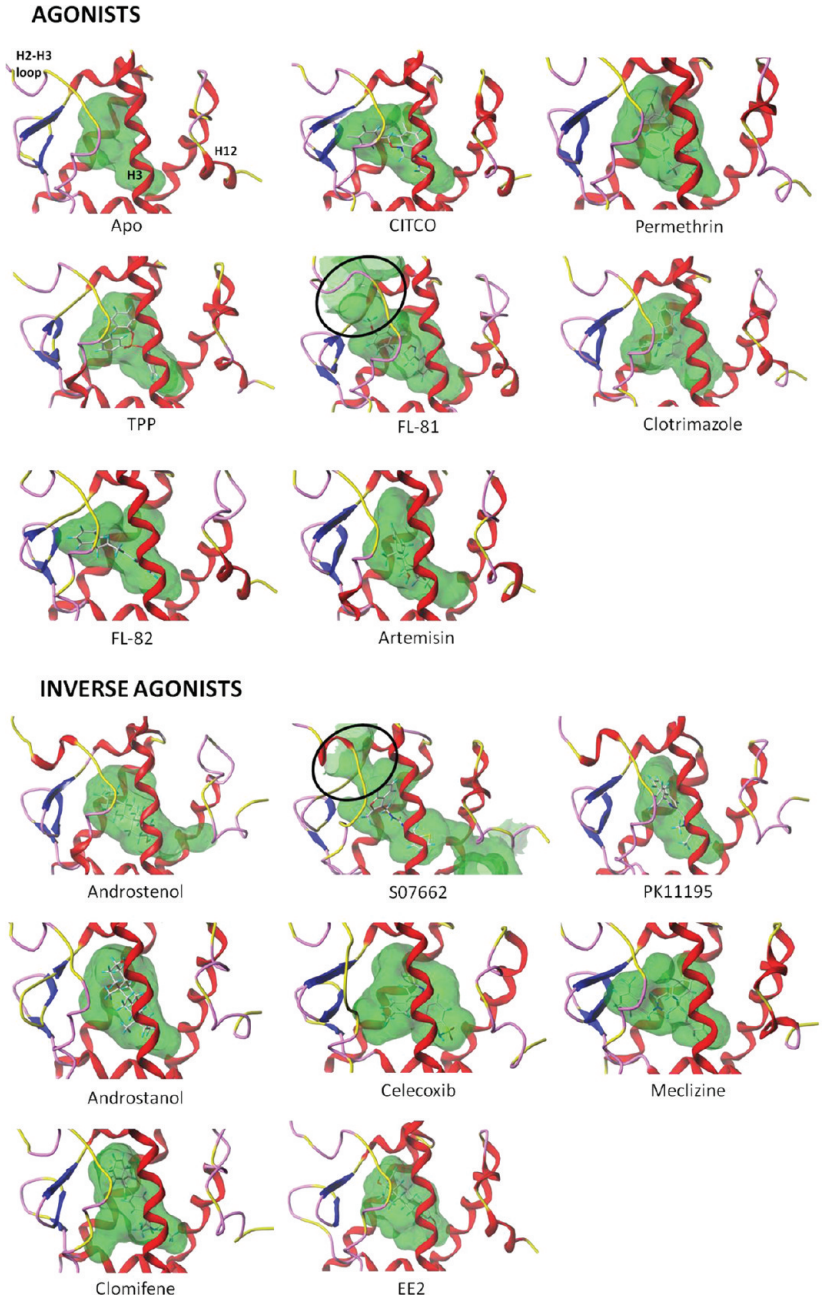

Figure 2. Ligand binding pockets of CAR with ligands at the end of 10 ns MDs. Connolly surfaces (calculated with SYBYL) are shown in green. Opening of the cavity, caused by the movement of the H2−H3 loop, is circled.

obtained with the *ptraj* module of AMBER10. The final rescoring was calculated as a single point calculation without minimization. Additionally, contact preference maps of ambiguous docking poses were inspected by using the Molecular Operating Environment (MOE; Chemical Computing Group Inc., Quebec, Canada), and the basis for selecting the best pose for each ligand was according to both binding energy and adequacy of the interaction fields.

Incorporation of the Corepressor Peptide. The crystal structure of peroxisome proliferator-activated receptor-gamma (PPARγ), which included the SMRT peptide (1KKQ),[18] was aligned with CAR docking poses by using the homology-based alignment of SYBYL 8.1 (Tripos, St. Louis, MO, USA). SMRT was then extracted from PPAR and merged onto the CAR coregulator surface (sequence alignment of the important parts of PPAR and CAR as well as the alignment of SMRT and NCoR are shown in the Supporting Information, Figure S1). To remove the steric clashes between CAR and SMRT, the interaction surface was minimized as described below.

Molecular Dynamics Simulations. Periodic water box simulations of 10 ns were made for selected dockings poses and for the corresponding empty human CAR LBD, all with added SMRT peptides, by using the *sander* program of AMBER10. Hydrogen atoms were added to protein atoms with the *xleap* module of the AMBER10 program. For the protein, force field parameters and partial charges from the ff99sb force field were used.[19] For the small molecules, the GAFF parameter assignments[20] were made by using the *antechamber* module, and the atom-centered partial charges were generated by using the AM1-BCC method.[21] Structures were solvated with a box of

dx.doi.org/10.1021/ci200432k | J. Chem. Inf. Model. 2012, 52, 457−464

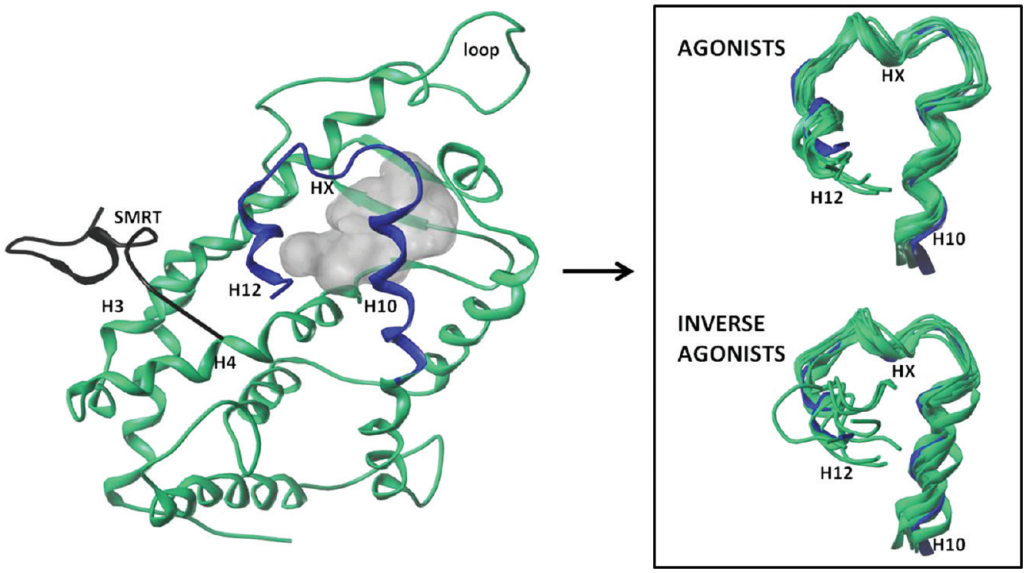

Figure 3. Position of H12 after the 10 ns MD. On the left, the backbone of apo CAR LBD is shown in green, the LBP in gray, and the SMRT peptide in black. The backbone of C-terminal residues of the LBD is in blue. On the right, the position of H12 in the presence of ligands has been compared. Apo is shown in blue, and ligand structures are in green.

TIP3P water molecules, and the structural crystal water molecules were included in the simulations. For the MD simulations, the water molecules and the hydrogens of the protein were first energy minimized for 1000 steps. Contacts between SMRT and H12 were relaxed by calculating an additional 5000 steps of minimization, using constraints for protein heavy atoms excluding SMRT and the last four residues of H12. The solvent box was heated to 300 K over 7.5 ps and then equilibrated for 50 ps at a constant temperature of 300 K and at a pressure of 1 atm. Subsequently, the entire simulation system was minimized for 1000 steps, and the temperature of the system was increased to 300 K over 7.5 ps and equilibrated for 300 ps by using a time step of 1.5 fs. The SHAKE algorithm was used to constrain the bonds involving hydrogen atoms to their equilibrium values.[22] Consequently, production NPT simulations of 10.0 ns were computed. The cutoff for Lennard-Jones interactions was 8 Å, and the particle mesh Ewald (PME) method was used for the treatment of electrostatic interactions.[23] The stability of the structures was checked from the RMS deviations, and the trajectories were analyzed for atomic positional fluctuation and protein secondary structure with the *ptraj* program of Amber Tools 1.3.[24] The final structures from the MD runs were visually examined with the assistance of the SYBYL software, and the Connolly surfaces of the LBPs were calculated by using the MOLCAD option of SYBYL-X 1.2 with a 1.6 Å probe radius (otherwise default settings were used).

MM-GBSA Binding Free Energy Calculation. To calculate the MM-GBSA binding free energy, MD simulations (see above) of 10 ns in explicit water were first performed for the human CAR LBD, which included bound ligands.[25] After removal of solvent water molecules, the separate 50 "snapshot" structures of complex, protein, and ligand were extracted from the molecular dynamics trajectories. It has been observed that a computation time of 1 ns and the single trajectory method provide fairly good estimates for the relative binding energies.[25−28] Therefore, the first set of snapshots was taken during the first nanosecond of the MD run. However, since the MD starting structure of CAR was that of an agonist-bound receptor, and certain regions of the structure seemed to change considerably in the presence of inverse agonists, another set of 50 snapshots was taken during the ninth nanosecond of the MD run. The average free energies of the extracted snapshots were then used to calculate binding free energies (ΔG) for the protein−ligand association ($\Delta G_{bind} = \Delta G_{complex} - \Delta G_{protein} - \Delta G_{ligand}$). The binding free energies (ΔG) of the protein−ligand complex can be calculated as a sum of the average molecular mechanical gas-phase energies (E_{MM}), solvation free energies (ΔG_{solv}), and entropy contributions ($T\Delta S$) ($\Delta G = E_{MM} + \Delta G_{solv} - T\Delta S$, where $\Delta G_{solv} = \Delta G_{GB} + \Delta G_{np}$). In this work, the molecular mechanical (E_{MM}) energies were calculated by using the *sander* program of AMBER10 with all protein pairwise interactions included and a dielectric constant (ε) of 1.

The solvation free energy (ΔG_{solv}) is the sum of electrostatic solvation, which is calculated by the finite difference solution of the generalized Born equation (ΔG_{GB}) with the *sander* program,[29] and nonpolar solvation energy (ΔG_{np}) calculated from the solvent-accessible surface area (SASA) term, which is calculated by using the LCPO-method embedded in the *sander* program.[30] The entropy term, due to the loss of degrees of freedom upon association, has been omitted because it is very demanding to calculate, and its value seldom converges.[28] Thus, it does not necessarily provide a further understanding for the ligand−protein interactions studied here.

Chemicals. All steroids were from Steraloids, Inc. (Newport, RI). The synthesis and characterization of compound FL-82 (5-benzyl-3-phenyl-4,5-dihydroisoxazole) has been previously described.[31] Preparation of compound FL-81[32] (5-(3,4-dimethoxybenzyl)-3-phenyl-4,5-dihydro-isoxazole) was performed using the same procedure[31] and characterized as follows: yield 78%, mp = 110.8−112.8 °C. ^{1}H NMR: δ 7.64 (m, 2 H), 7.38 (m, 3 H), 6.81 (m, 3 H), 4.97 (m, 1 H), 3.88 (s, 3 H), 3.86 (s, 3 H), 3.32 (dd, 1 H, J = 16.6, 10.3), 3.09 (dd, 1 H, J = 14.0, 6.2), 3.01 (dd, 1 H, J = 16.6, 7.9), 2.85 (dd, J = 14.0, 6.8). ^{13}C NMR: δ 156.5, 149.0, 147.9 (3 s), 130.0 (d), 129.7, 129.5 (2 s), 128.7, 126.6, 121.4, 112.6, 111.3, 82.0 (6 d), 55.9, 55.9 (2 q), 40.6, 39.3 (2 t). Triphenyl phosphate (TPP) was synthesized as described,[33] and S07662 as described.[16]

dx.doi.org/10.1021/ci200432k | J. Chem. Inf. Model. 2012, 52, 457−464

Table 2. van der Waals Interactions between H11 (Y326 and I330) and H12 (L343 and L346) As Well As H Bonds between H11 and H12 from the Final Structures of the 10 ns MD runs (Cut-off Distance for van der Waals Interactions = 4 Å)

	Y326–L343	Y326–I346	I330–L343	I330–I346	H bonds
Apo	-[a]	-	●[b]	-	-
CITCO	●	-	●	-	E324–S348 (sc[c]-sc)
FL-82	●	-	●	-	Q331–C347 (sc-bb[d])
FL-81	●	-	●	-	-
Permethrin	●	-	●	-	-
Clotrimazole	●	-	●	-	-
TPP	●	-	●	-	Q331–Q344 (sc-sc)
Artemisin	●	-	●	-	-
EE2	●	-	●	-	-
Androstanol	●	-	●	-	-
Androstenol	-	-	-	●	-
PK11195	-	●	-	●	-
S07662	-	-	●	●	-
Clomifen	●	●	●	●	Q331–Q344 (sc-bb)
Celecoxib	-	-	-	-	-
Meclizine	●	-	●	-	E324–S348 (sc-sc)
					Q331–S348 (sc-bb)

[a]No interaction. [b]van der Waals interaction. [c]Side chain. [d]Backbone.

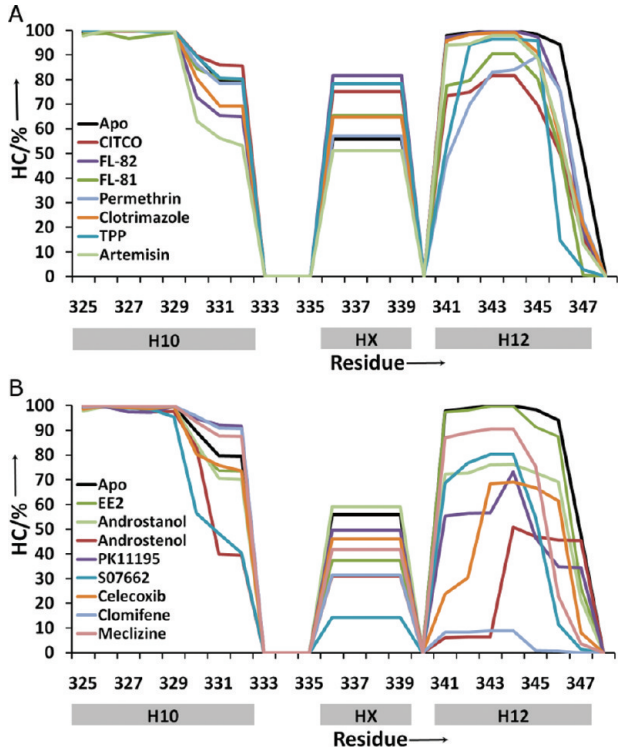

Figure 4. Helical conformation (HC; % of the MD time) of the C-terminal residues of CAR during MD simulations.

Meclizine was a kind gift from H. Wang (University of Maryland, MD) and T. Sueyoshi (NIEHS, NC). Celecoxib was purchased from Cayman Chemicals (Ann Arbor, MI); other chemicals were at least of analytical grade from Sigma Aldrich. All chemicals were dissolved and diluted in DMSO.

***In Vitro* Assays and Cell Culture.** Activation of hCAR was measured in C3A hepatoma cells using reporter gene assays. Cell culture and reporter gene assays have been described in detail.[10] NCoR recruitment was studied by using mammalian 2-hybrid assays in C3A cells and has been described.[15] Cytotoxicity of the compounds used here was measured using an MTT test,[34] and the data are available in the Supporting Information (Table S1).

RESULTS AND DISCUSSION

Seven agonists and eight inverse agonists (Table 1; inverse agonism of meclizine is controversial[35,36]) were docked to the human CAR LBP by using the Gold 4.0 docking suite. The side chains of F161 and Y224 were allowed to move freely.[12] Since the fitness scores provided by the docking suites are not always able to select the correct binding configuration, we applied additional methods to analyze the docking poses. We calculated the molecular interaction fields of the ligands by using the MOE modeling suite and rescored the poses by calculating the theoretical single point binding energies for ligands with the GBSA module of the Amber 10 MD package. The ligand poses for MDs were then selected according to three criteria: Gold fitness score, GBSA score, and the inspection of the molecular interaction fields.

Prior to the MDs, the SMRT peptide was inserted into the CAR LBD by superimposing the hCAR LBD to the PPARγ/SMRT cocrystal structure[18] and then merging SMRT onto the coregulator groove of the CAR. The MDs were run for 10 ns, and the trajectories were analyzed with Amber. The atomic positional fluctuation (APF) of the backbone atoms during MD showed how agonists seemed to have very little or no effect on the loop between H2 and H3 (Figure 1a), which is probably the most flexible part of the CAR LBD with high APFs (Supporting Information, Figure S2). Many inverse agonists, on the other hand, tended to destabilize this loop (Figure 1b). The loop is presumably one of the ligand entry sites,[37,38] and destabilization resulted in an opening of the ligand binding cavity with the most efficacious inverse agonist S07662 and the agonist FL-81 (Figure 2). In this respect, FL-81 was an exception from the other agonists, and this probably causes the more modest activity compared to its relative compound FL-82.

The C-terminal residues of CAR (Figure 1c and d), which are essential in stabilizing the position of H12, were stabilized by agonists but moved more in the presence of inverse agonists. This result is as expected: the H12 has to move from the active position, in which it is at the beginning of the MD, in order to accommodate a corepressor. In many NRs, the movement of H12 is quite large, and in the presence of corepressors H12 is oriented completely away from the LBD.[3,39] Human CAR has quite a short H12, as well as a barrier of side chains that prevent ligands from clearly pushing the H12 away. Therefore, as previously discussed, the subtle movement of H12 toward H10 elicited by most inverse agonists (Figure 3 and Supporting Information, Figure S3) might be sufficient for corepressor binding.[16] Human CAR is not the only NR where such a movement of H12 toward H10 is seen. The position of H12 in the presence of an antagonist can vary significantly, and in the progesterone receptor, (PR) the yielding movement of H12 seems to the same direction as was seen in hCAR.[39]

Only the movement of H12 toward H10 seems to favor the binding of SMRT. This movement causes changes in the stabilizing van der Waals interactions between H12 and H10 (Table 2). On the other hand, it seems that if elongation of H12 without movement toward H10 or an outward movement of H12 is seen in the MDs, then this movement could predict

dx.doi.org/10.1021/ci200432k | J. Chem. Inf. Model. 2012, 52, 457–464

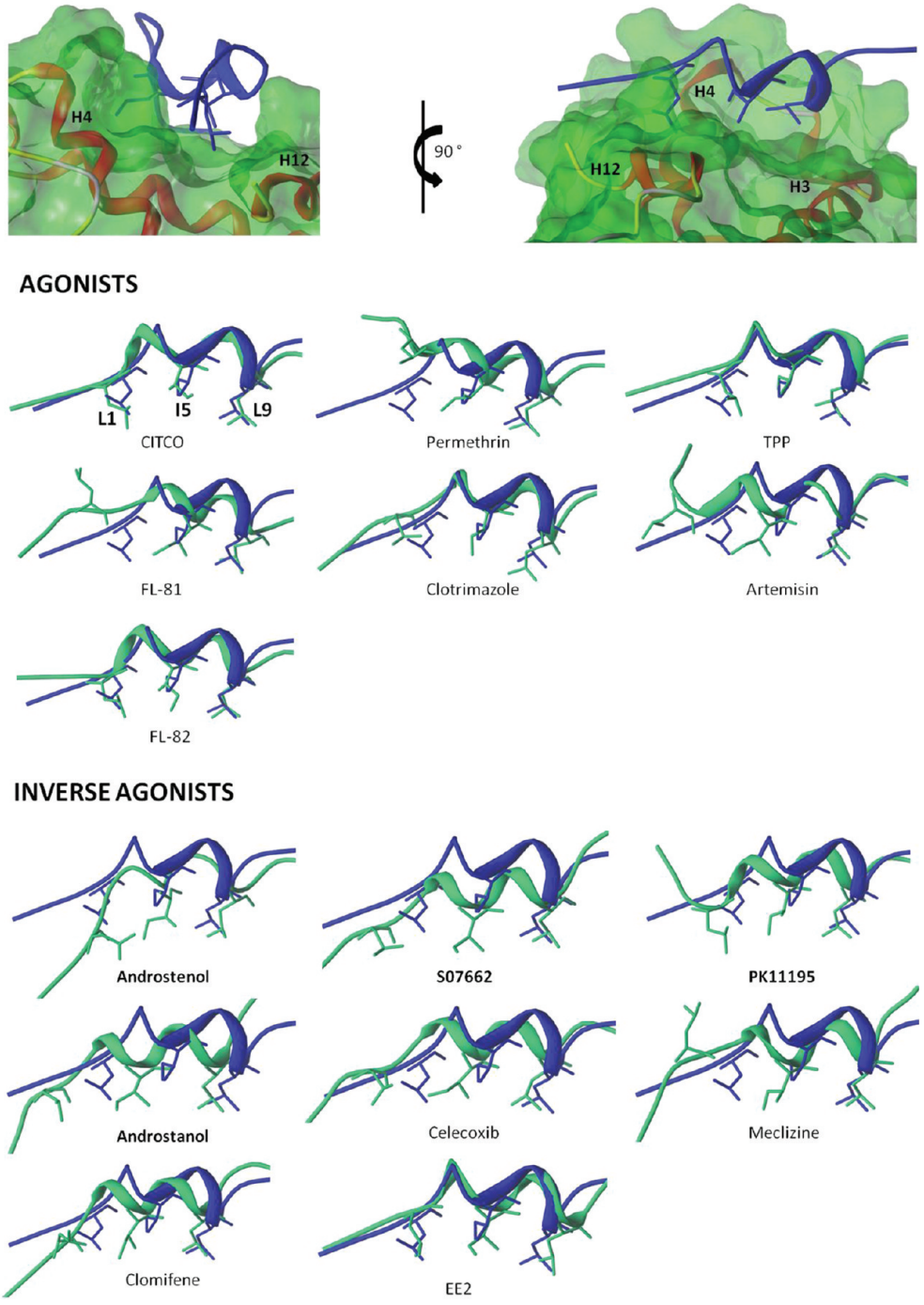

Figure 5. The SMRT peptide on the CAR LBD. On top is the coregulator groove of the apo-structure with SMRT, and below are shown the most important nuclear receptor interaction motif residues L1, I5, and L9 (boldface) of SMRT on the liganded structures (green), compared to the apo-structure (blue). The motif of the SMRT peptide used here is **L**EAII**I**RKA**L** (residues 2329−2337 in RefSeq).

compromised NCoR/SMRT binding (Table 1 and Supporting Information, Figure S3). In the case of clomifene and meclizine, hydrogen bond(s) formed between H12 and H10 probably prevent the H12 from giving way to a corepressor peptide (Tables 1 and 2).

The existence of a short rigid helix between H10 and H12, called HX, may retain H12 in the active position and be one of the features that cause the high constitutive activity of CAR.[6] Thus, any movement of H12 has to be enabled by the flexibility of HX. Indeed, this seems to be the case. We analyzed the stability of the helical conformation of the α helices during the MDs. Figure 4 shows that the helical conformation of HX seems to be less stable in the presence of inverse agonists than in the apo structure or in the presence of agonists. On the basis of the mutational and HDX data, a similar feature was recently reported also for the mouse CAR.[40] Unlike in our previous study,[16] due to the presence of SMRT, all of the ligands seemed to reduce the helical content of H12.

In Figure 5, the positions of the most important SMRT residues[18] (Leu2329, Ile2333, and Leu2337) for NR binding are shown. None of these three residues can solely determine the binding of SMRT, but their overall proper fit is essential for

dx.doi.org/10.1021/ci200432k | J. Chem. Inf. Model. 2012, 52, 457−464

the binding. In the presence of androstanol, androstenol, PK11195, and S07662, all three residues were able to fit deep in the groove, due to the yielding of H12 (Supporting Information, Figure S3), and enabled an efficient binding of SMRT (Figure 5). This was also seen in the high *in vitro* NCoR binding (Table 1). Either other ligands induced no changes in the position of H12 compared to apo (EE2) or the movement of H12 was not into a favorable direction (Supporting Information, Figure S3) which prevented the N-terminus of SMRT from binding properly (celecoxib, clomifene, and meclizine; Figure 5). These ligands induced no NCoR either (Table 1). The considerable differences seen between very similar androstanol and androstenol are caused by the fact that most probably their binding conformations differ considerably. In our dockings, the binding pose for androstenol was unambiguous, but that of androstanol had to be determined by energy calculation and grid fields, as described in the Experimental Section. The A-ring of androstenol was oriented toward H12, whereas androstenol was oriented in an opposite fashion with the D-ring pointing to H12 (Figure 2).

In our previous study, we found a good correlation between the activity of agonists and the theoretical ligand interaction energies that were calculated with the MM-GBSA method with 1 ns MDs.[15] Such a short MD for these energy calculations is justifiable when studying similar types of ligands.[41] However, this method could not distinguish between agonists and inverse agonists. In the present study, we calculated ligand interaction energies with MM-GBSA at two time frames, during the first and the ninth nanosecond of the MD (Table 1). Since the starting conformations of the MDs are those of an active receptor, potent inverse agonists tended to change the conformation of the LBD, which was reflected in a change with the ligand−protein interaction energy. Perhaps due to the fact that the ratio between entropic (not estimated here[28]) and enthalpic contributions to ligand binding may vary from one ligand to another, the direction of this change was not consistent. The binding of the corepressor was not always reflected by the improvement of the binding energy; rather, the opposite change could also be seen.

CONCLUSIONS

In conclusion, we were able to elucidate structural changes of hCAR LBD induced by the inverse agonists by including a corepressor peptide SMRT in the MDs. Due to the structural features contributing to the constitutive activity, merely adding a ligand in the hCAR pocket did not elicit explicit changes in the LDB structure. Major structural differences in the simulations were only seen when the hCAR LBD was occupied by inverse agonists and the coregulator groove by a corepressor peptide. This model will be further validated as new inverse agonists for CAR are being found. Furthermore, some of the inverse agonists (i.e., clomifene and celecoxib) may have ligand-specific corepressors because the decreased hCAR activity could not be explained by NCoR recruitment or by simulated SMRT binding.

ASSOCIATED CONTENT

Supporting Information

Table S1 with the cytotoxicity data. Figure S1 showing the alignment of the important parts of hCAR and PPARγ, as well as alignment of SMRT and NCoR peptides. Figure S2 showing the atomic positional fluctuation (APF) of the entire ligand binding domain of CAR during the MD. Figure S3 showing the position of H12 separately with each of the studied ligands. This information is available free of charge via the Internet at http://pubs.acs.org/.

AUTHOR INFORMATION

Corresponding Author

*Tel.: +358 40 3552520 (J.J.), +358 400 165489 (T.L.). Fax: +358 17 162424 (J.J.), +358 17 162424 (T.L.). E-mail: Johanna.Jyrkkärinne@uef.fi (J.J.), Tuomo.Laitinen@uef.fi (T.L.).

Notes

The authors declare no competing financial interest.

ACKNOWLEDGMENTS

Ms. Lea Pirskanen is thanked for technical assistance in the biological experiments. This work was supported in part by Biocenter Finland (Laitinen, Jyrkkärinne). The authors also thank CSC−IT Center for Science Ltd. (Espoo, Finland) for providing computational resources.

REFERENCES

(1) Timsit, Y. E.; Negishi, M. CAR and PXR: the xenobiotic-sensing receptors. *Steroids* **2007**, *72*, 231−246.

(2) Gao, J.; Xie, W. Pregnane x receptor and constitutive androstane receptor at the crossroads of drug metabolism and energy metabolism. *Drug. Metab. Dispos.* **2010**, *38*, 2091−2095.

(3) Bain, D. L.; Heneghan, A. F.; Connaghan-Jones, K. D.; Miura, M. T. Nuclear receptor structure: implications for function. *Annu. Rev. Physiol.* **2007**, *69*, 201−220.

(4) Kremoser, C.; Albers, M.; Burris, T. P.; Deuschle, U.; Koegl, M. Panning for SNuRMs: using cofactor profiling for the rational discovery of selective nuclear receptor modulators. *Drug Discovery Today* **2007**, *12*, 860−869.

(5) Mäkinen, J.; Reinisalo, M.; Niemi, K.; Viitala, P.; Jyrkkärinne, J.; Chung, H.; Pelkonen, O.; Honkakoski, P. Dual action of oestrogens on the mouse constitutive androstane receptor. *Biochem. J.* **2003**, *376*, 465−472.

(6) Xu, R. X.; Lambert, M. H.; Wisely, B. B.; Warren, E. N.; Weinert, E. E.; Waitt, G. M.; Williams, J. D.; Collins, J. L.; Moore, L. B.; Willson, T. M.; Moore, J. T. A structural basis for constitutive activity in the human CAR/RXRalpha heterodimer. *Mol. Cell* **2004**, *16*, 919−928.

(7) Shan, L.; Vincent, J.; Brunzelle, J. S.; Dussault, I.; Lin, M.; Ianculescu, I.; Sherman, M. A.; Forman, B. M.; Fernandez, E. J. Structure of the murine constitutive androstane receptor complexed to androstenol: a molecular basis for inverse agonism. *Mol. Cell* **2004**, *16*, 907−917.

(8) Jyrkkärinne, J.; Windshügel, B.; Rönkkö, T.; Tervo, A. J.; Küblbeck, J.; Lahtela-Kakkonen, M.; Sippl, W.; Poso, A.; Honkakoski, P. Insight into ligand-elicited activation of human constitutive androstane receptor based on novel agonists and three-dimensional quantitative structure-activity relationship. *J. Med. Chem.* **2008**, *51*, 7181−7192.

(9) Repo, S.; Jyrkkärinne, J.; Pulkkinen, J. T.; Laatikainen, R.; Honkakoski, P.; Johnson, M. S. Ligand specificity of constitutive androstane receptor as probed by induced-fit docking and mutagenesis. *J. Med. Chem.* **2008**, *51*, 7119−7131.

(10) Küblbeck, J.; Jyrkkärinne, J.; Poso, A.; Turpeinen, M.; Sippl, W.; Honkakoski, P.; Windshügel, B. Discovery of substituted sulfonamides and thiazolidin-4-one derivatives as agonists of human constitutive androstane receptor. *Biochem. Pharmacol.* **2008**, *76*, 1288−1297.

(11) Windshügel, B.; Jyrkkärinne, J.; Vanamo, J.; Poso, A.; Honkakoski, P.; Sippl, W. Comparison of homology models and x-ray structures of the nuclear receptor CAR: assessing the structural basis of constitutive activity. *J. Mol. Graphics Modell.* **2007**, *25*, 644−657.

(12) Windshügel, B.; Jyrkkärinne, J.; Poso, A.; Honkakoski, P.; Sippl, W. Molecular dynamics simulations of the human CAR ligand-binding

domain: deciphering the molecular basis for constitutive activity. *J. Mol. Model.* **2005**, *11*, 69−79.
(13) Jyrkkärinne, J.; Windshügel, B.; Mäkinen, J.; Ylisirniö, M.; Peräkylä, M.; Poso, A.; Sippl, W.; Honkakoski, P. Amino acids important for ligand specificity of the human constitutive androstane receptor. *J. Biol. Chem.* **2005**, *280*, 5960−5971.
(14) Jyrkkärinne, J.; Mäkinen, J.; Gynther, J.; Savolainen, H.; Poso, A.; Honkakoski, P. Molecular determinants of steroid inhibition for the mouse constitutive androstane receptor. *J. Med. Chem.* **2003**, *46*, 4687−4695.
(15) Küblbeck, J.; Laitinen, T.; Jyrkkärinne, J.; Abel, T.; Kortelainen, T.; Uusitalo, J.; Korjamo, T.; Honkakoski, P.; Molnár, F. Use of comprehensive screening methods to detect selective human CAR activators. *Biochem. Pharmacol.* **2011**, *82*, 1994−2007.
(16) Küblbeck, J.; Jyrkkärinne, J.; Molnár, F.; Kuningas, T.; Patel, J.; Windshügel, B.; Nevalainen, T.; Laitinen, T.; Sippl, W.; Poso, A.; Honkakoski, P. New *in vitro* tools to study human CAR biology: discovery and comparison of human CAR inverse agonists. *Mol. Pharm.* **2011**, *8*, 2424−2433.
(17) Case, D. A.; Darden, T. A.; Cheatham, T. E., III; Simmerling, C. L.; Wang, J.; Duke, R. E.; Luo, R.; Crowley, M.; Walker, R. C.; Zhang, W.; Merz, K. M.; Wang, B.; Hayik, S.; Roitberg, A.; Seabra, G.; Kolossváry, I.; Wong, K. F.; Paesani, F.; Vanicek, J.; Wu, X.; Brozell, S. R.; Steinbrecher, T.; Gohlke, H.; Yang, L.; Tan, C.; Mongan, J.; Hornak, V.; Cui, G.; Mathews, D. H.; Seetin, M. G.; Sagui, C.; Babin, V.; Kollman, P. A. *AMBER 10*; University of California: San Francisco, 2008.
(18) Xu, H. E.; Stanley, T. B.; Montana, V. G.; Lambert, M. H.; Shearer, B. G.; Cobb, J. E.; McKee, D. D.; Galardi, C. M.; Plunket, K. D.; Nolte, R. T.; Parks, D. J.; Moore, J. T.; Kliewer, S. A.; Willson, T. M.; Stimmel, J. B. Structural basis for antagonist-mediated recruitment of nuclear co-repressors by PPARalpha. *Nature* **2002**, *415*, 813−817.
(19) Hornak, V.; Abel, R.; Okur, A.; Strockbine, B.; Roitberg, A.; Simmerling, C. Comparison of multiple amber force fields and development of improved protein backbone parameters. *Proteins* **2006**, *65*, 712−725.
(20) Wang, J.; Wolf, R. M.; Caldwell, J. W.; Kollman, P. A.; Case, D. A. Development and testing of a general amber force field. *J. Comput. Chem.* **2004**, *25*, 1157−1174.
(21) Jakalian, A.; Bush, B. L.; Jack, D. B.; Bayly, C. I. Fast, efficient generation of high-quality atomic charges. AM1-BCC Model: I. Method. *J. Comput. Chem.* **2000**, *21*, 132−146.
(22) Ryckaert, J. P.; Ciccotti, G.; Berendsen, H. J. C. Numerical integration of the cartesian equations of motion of a system with constraints: molecular dynamics of n-alkanes. *J. Comput. Physics* **1977**, *23*, 327−341.
(23) Darden, T.; York, D.; Pedersen, L. mesh Ewald: An N.log(N) method for ewald sums in large systems. *J. Chem. Phys.* **1993**, *12*, 10089−10092.
(24) Case, D. A.; Cheatham, T. E. III; Darden, T.; Gohlke, H.; Luo, R.; Merz, K. M. Jr.; Onufriev, A.; Simmerling, C.; Wang, B.; Woods, R. The amber biomolecular simulation programs. *J. Comput. Chem.* **2005**, *26*, 1668−1688.
(25) Kollman, P. A.; Massova, I.; Reyes, C.; Kuhn, D.; Huo, S.; Chong, L.; Lee, M.; Lee, T.; Duan, Y.; Wang, W.; Donini, O.; Cieplak, P.; Srinivasan, J.; Case, D. A.; Cheatham, T. E. III. Calculating structures and free energies of complex molecules: combining molecular mechanics and continuum models. *Acc. Chem. Res.* **2000**, *33*, 889−897.
(26) Kuhn, B.; Kollman, P. A. Binding of a diverse set of ligands to avidin and streptavidin: an accurate quantitative prediction of their relative affinities by a combination of molecular mechanics and continuum solvent models. *J. Med. Chem.* **2000**, *43*, 3789−3791.
(27) Laitinen, T.; Kankare, J. A.; Peräkylä, M. Free energy simulations and MM-PBSA analyses on the affinity and specificity of steroid binding to antiestradiol antibody. *Proteins* **2004**, *55*, 34−43.
(28) Gohlke, H.; Kuhn, L. A.; Case, D. A. Change in protein flexibility upon complex formation: analysis of ras-raf using molecular dynamics and a molecular framework approach. *Proteins* **2004**, *56*, 322−337.
(29) Onufriev, A.; Bashford, D.; Case, D. A. Modification of the generalized born model suitable for macromolecules. *J. Phys. Chem. B* **2000**, *104*, 3712−3720.
(30) Weiser, J.; Shenkin, P. S.; Still, W. C. Approximate solvent-accessible surface areas from tetrahedrally directed neighbor densities. *J. Comput. Chem.* **1999**, *20*, 217−230.
(31) Pulkkinen, J. T.; Honkakoski, P.; Peräkylä, M.; Berczi, I.; Laatikainen, R. Synthesis and evaluation of estrogen agonism of diaryl 4,5-dihydroisoxazoles, 3-hydroxyketones, 3-methoxyketones, and 1,3-diketones: a compound set forming a 4d molecular library. *J. Med. Chem.* **2008**, *51*, 3562−3571.
(32) D'Alcontres, G. S. Nitrile oxides. VIII. Nitrile oxides and unsaturated phenols. *Gazz. Chim. It.* **1952**, *82*, 832−827.
(33) Honkakoski, P.; Palvimo, J. J.; Penttilä, L.; Vepsäläinen, J.; Auriola, S. Effects of triaryl phosphates on mouse and human nuclear receptors. *Biochem. Pharmacol.* **2004**, *67*, 97−106.
(34) Mosmann, T. Rapid colorimetric assay for cellular growth and survival: application toproliferation and cytotoxicity assays. *J. Immunol. Methods* **1983**, *65*, 55−63.
(35) Huang, W.; Zhang, J.; Wei, P.; Schrader, W. T.; Moore., D. D. Meclizine is and agonist ligand for mouse constitutive androstane receptor (CAR) and an inverse agonist for human CAR. *Mol. Endocrinol.* **2004**, *18*, 2402−2408.
(36) Lau, A. J.; Yang, G.; Rajaraman, G.; Baucom, C. C.; Chang, T. K. Differential effect of meclizine on the activity of human pregnane x receptor and constitutive androstane receptor. *J. Pharmacol. Exp. Ther.* **2011**, *336*, 816−826.
(37) Renaud, J. P.; Rochel, N.; Ruff, M.; Vivat, V.; Chambon, P.; Gronemeyer, H.; Moras, D. Crystal structure of the RAR-gamma ligand-binding domain bound to all-trans retinoic acid. *Nature* **1995**, *378*, 681−689.
(38) Martínez, L.; Sonoda, M. T.; Webb, P.; Baxter, J. D.; Skaf, M. S.; Polikarpov, I. Molecular dynamics simulations reveal multiple pathways of ligand dissociation from thyroid hormone receptors. *Biophys. J.* **2005**, *89*, 2011−2023.
(39) Zhou, J.; Liu.; Geng, B. G.; Wu, J. H. Study of the impact of the T877A mutation on ligand-induced helix-12 positioning of the androgen receptor resulted in design and synthesis of novel antiandrogens. *Proteins* **2010**, *78*, 623−637.
(40) Wright, E.; Busby, S. A.; Wisecarver, S.; Vincent, J.; Griffin, P. R.; Fernandez, E. J. Helix 11 Dynamics is critical for constitutive androstane receptor activity. *Structure* **2011**, *19*, 37−44.
(41) Hou, T.; Wang, J.; Li, Y.; Wang, W. Assessing the performance of the MM/PBSA and MM/GBSA methods. 1. The accuracy of binding free energy calculations based on molecular dynamics simulations. *J. Chem. Inf. Model.* **2011**, *51*, 69−82.